

RESEARCH ARTICLE

WILEY

Urolithin A: A promising selective estrogen receptor modulator and 27-hydroxycholesterol attenuator in breast cancer

Ravindran Vini^{1,2}  | Vishnu Sunil Jaikumar³  | Viji Remadevi^{1,2} |
Swathy Ravindran¹ | Juberiya M. Azeez^{1,2} | Anjana Sasikumar¹ |
Shankar Sundaram⁴ | Sreeharshan Sreeja¹ 

¹Cancer Research Program, Rajiv Gandhi Centre for Biotechnology (RGCB), Thiruvananthapuram, India

²Research Centre, University of Kerala, Thiruvananthapuram, India

³Animal Research Facility, Rajiv Gandhi Centre for Biotechnology (RGCB), Thiruvananthapuram, India

⁴Department of Pathology, Government Medical College, Kottayam, India

Correspondence

Sreeharshan Sreeja, Rajiv Gandhi Centre for Biotechnology (RGCB), Thycaud PO, Thiruvananthapuram, Kerala 695014, India.
Email: ssreeja@rgcb.res.in

Funding information

Science and Engineering Research Board, Grant/Award Number: EMR/000557; Department of Biotechnology, Grant/Award Number: BT/01/CEIB/01/CB/2016

Abstract

27-hydroxycholesterol (27-HC) is an oxysterol that acts as an endogenous selective estrogen receptor modulator (SERM), and its adverse effects on breast cancer via the estrogen receptor (ER) have provided new insights into the pathology of cholesterol-linked breast cancer. Our earlier in vitro experiments showed that the methanolic extract of pomegranate could exhibit SERM properties and compete with 27-HC. The major constituents of pomegranate are ellagitannins and ellagic acid, which are converted into urolithins by the colonic microbiota. In recent years, urolithins, especially urolithin A (UA) and urolithin B (UB), have been reported to have a plethora of advantageous effects, including antiproliferative and estrogenic activities. In this study, we attempted to determine the potential of urolithins in antagonizing and counteracting the adverse effects of 27-HC in breast cancer cells. Our findings suggested that UA had an antiproliferative capacity and attenuated the proliferative effects of 27-HC, resulting in subsequent loss of membrane potential and apoptosis in breast cancer cells. Further, UA induced estrogen response element (ERE) transcriptional activity and modulated estrogen-responsive genes, exhibiting a SERM-like response concerning receptor binding. Our in vivo hollow fiber assay results showed a loss of cell viability in breast cancer cells upon UA consumption, as well as a reduction in 27-HC-induced proliferative activity. Additionally, it was shown that UA did not induce uterine proliferation or alter blood biochemical parameters. Based on these findings, we can conclude that UA has the potential to act as a potent estrogen receptor alpha (ER α) modulator and 27-HC antagonist. UA is safe to consume and is very well tolerated. This study further opens up the potential of UA as ER modulator and its benefits in estrogen-dependent tissues.

KEYWORDS

27-hydroxycholesterol (27-HC), breast cancer, selective estrogen receptor modulator (SERM), urolithin A

1 | INTRODUCTION

The revelation of a potential link between breast cancer and cholesterol came to the forefront with the discovery of 27-hydroxycholesterol (27-HC), a cholesterol metabolite that functions as an endogenous selective estrogen receptor modulator (SERM) (Umetani et al., 2007). This metabolite has been shown to promote breast cancer proliferation and metastasis in both in vitro and in vivo (Nelson, 2018; Wu et al., 2013). In addition to its impact on breast cancer, 27-HC is also involved in the modulation of the liver X receptor and immune cells (Baek et al., 2017, 2021; Ma et al., 2020) and has been found to induce methylation changes in breast cancer cells (Vini et al., 2022) to bring breast cancer progression and metastasis. At the clinical level, higher levels of the enzyme CYP27A1, responsible for synthesizing 27-HC, have been correlated with increased tumor grade and aggression. Interestingly, reduced expression of CYP7B1, the 27-HC-catabolizing enzyme in tumors, has been associated with poorer patient survival (Asghari & Umetani, 2020). It is worth noting that 27-HC has been found to exert deleterious effects on other body parts, including hormone-responsive tissues (Dias et al., 2018; Gibson et al., 2018; Ismail et al., 2017; Kim et al., 2021; Lee et al., 2014; Nelson et al., 2011; Revilla et al., 2019). Estrogen receptor alpha (ER α) is involved in driving neoplasia in ER positive breast cancer and therefore represents a valid therapeutic target. Endocrine therapy aims to reduce ER activity or receptor expression levels in breast cancer cells. However, the clinical implications of 27-HC and its contribution to breast cancer need further elucidation. A shred of preclinical evidence suggests that 27-HC stimulates breast cancer proliferation via ERs. Hence, this study attempted to explore whether the use of an exogenous ligand could counteract or reduce the effect of 27-HC on breast cancer proliferation. Tamoxifen, a SERM, is typically prescribed as a first-line treatment for ER-positive breast cancer to block the estrogen-stimulated proliferation of breast tumor cells. However, tamoxifen possesses tissue-selective agonist properties, which can also induce estrogen-like stimulation of tumors in some breast cancer patients at the onset of tamoxifen therapy (Mottamal et al., 2021). This partial agonistic activity limits its therapeutic efficacy due to its mixed action on the ER in different tissues. Consequently, many side effects are observed in the clinical and laboratory animal models (Mottamal et al., 2021). Our earlier experiments have demonstrated that the methanolic extract of pomegranate could act as an effective SERM, impeding breast cancer proliferation while retaining the positive effects on the cardiovascular system, and without causing endometrial thickening, unlike tamoxifen (Sreeja et al., 2012). Our laboratory has also shown that the extract could antagonize the proliferative activity of 27-HC (Vini et al., 2016). Pomegranates are rich in polyphenols (Sreekumar et al., 2014) and ellagitannins, which are broken down by intestinal microbiota to ellagic acid and urolithins inside

the body (García-Villalba et al., 2019; Vini et al., 2016). After consumption of ellagitannin-rich food, the primary metabolites detected in plasma are urolithin A (UA) and urolithin B (UB). Over the past decade, numerous studies have revealed that urolithins offer a plethora of health benefits, including protection against age-related muscle deterioration (Ryu et al., 2016; Singh et al., 2022); improving cardiovascular health; antiproliferative effects in breast, endometrial, bladder, and prostate cancer; and protection of the brain. Preliminary research (Larrosa, Tomás-Barberán, & Espin, 2006; Larrosa, González-Sarrías, et al., 2006; Skledar et al., 2019) indicated the potential for urolithins to serve as ER modulators, albeit more concrete evidence is required. We have previously proposed, urolithins could function as endocrine modulators (Vini et al., 2022). This study aimed to determine whether urolithins have the ability to bind to ER α and reduce the proliferative activity of 27-HC in breast cancer.

2 | MATERIALS AND METHODS

2.1 | Cell culture

Breast cancer cells, MCF-7, T47D, MDA-MB-231, and MCF-10A, were used (American Type Culture Collection [ATCC]). The passage number of the cell lines were between 2 and 10. MCF-7, T47D, and MDA-MB-231 were cultured in DMEM (Sigma Cat# D1152) supplemented with 10% Fetal Bovine Serum (FBS) and 1% penicillin and streptomycin (HiMedia, Cat# A002A) at 37°C with 5% CO₂. MCF-10A were cultured in MEBM supplemented with growth factors (MEGM-Lonza CC-4136). The cells were maintained in phenol-red-free DMEM (Sigma Cat# D1152) supplemented with 5% charcoal-stripped serum 72 h prior to treatment. The cells were maintained in a 37°C incubator with 5% CO₂ and 85% humidity. The experiments performed were not randomized/blinded.

2.2 | MTT assay

The 3-(4, 5-dimethylthiazolyl)-2, 5-diphenyltetrazolium bromide (MTT; Sigma-Aldrich Cat# 475989) assay was used to measure cell viability. Briefly, cells were plated at a density of 5000 cells/well in 96-flat-bottomed-well plates. Once the cells attained the morphology, they were pre-treated with 5% CTS low phenol-red-free medium. The cells were further treated with vehicle control (DMSO) or different concentrations of urolithin A (UA) and urolithin B (UB) for different time points, 24, 48, 72, and 96 h (1–100 μ M). Pure compounds, urolithin A (UA) (SC-475514A) and urolithin B (UB) (SC-475547), were purchased from Chemcruz. After treatment, the medium was replaced with MTT dissolved at a final concentration of 0.5 mg/mL in, phenol-red-free medium

and incubated for 4 h at 37°C. The MTT-formazan crystals were solubilized in lysis buffer (20% sodium dodecyl sulfate in 50% dimethylformamide), and the optical density was calculated as the difference between the absorbance at 570 nm and the absorbance at 630 nm and normalized to the respective controls. Cell survival was expressed as a percentage over the untreated control. Cell survival (CS) was calculated as $(OD \text{ drug-exposed cells} / \text{mean OD control cells}) \times 100$.

2.3 | Measurement of mitochondrial membrane potential

Cells were treated with UA or UB alone at different (25, 40, and 50 μM) concentrations and in combination with 27-HC (1 μM) for 72 h. After treatments, cells were trypsinized, and the cell pellets were resuspended and incubated with 50 nM tetramethylrhodamine methyl ester (TMRM Invitrogen 1853377) in phenol-red-free DMEM for 15 min. The cells were filtered and analyzed by Flow cytometry using a 488 nm laser for excitation and a 570 ± 10 nm emission filter for detection.

2.4 | Annexin-PI staining

Cells seeded in 6-well plates were treated with UA at different concentrations (25, 40, and 50 μM) or UA in combination with 27-HC (1 μM) for 72 h for and assessed for apoptosis by using fluorescein-isothiocyanate (FITC)-conjugated annexin V/PI assay kit. Briefly, treated cells were centrifuged at 1200 rpm for 5 min, washed twice with ice-cold PBS, resuspended in 500 μL binding buffer, and stained with 10 μL FITC-conjugated annexin V (10 mg/mL) and incubated for 10 min at room temperature (RT) in the dark. This was followed by incubation with PI (0.5 mg/mL) for 5 min in the dark. The filtered cells were analyzed using Flow Cytometer (BD Facsaria). Apoptosis was evaluated as described previously (Mbaveng et al., 2019). The results were analyzed and represented by using FlowJo software.

2.5 | BrdU cell proliferation assay

The rate of proliferation of cells was determined as the rate of incorporation of bromodeoxyuridine (BrdU) into cellular nucleic acids using the BrdU proliferation assay kit (Biovision K306). The cells were seeded in a 96-well plate at a density of 3000 cells/well. The cells were further treated with different concentrations of UA (40 μM) alone and in combination with 27-HC (1 μM) for 48 h. The cells were then pulsed with BrdU (100 M) 3 h before termination of the treatment to allow incorporation of the compound during the S-phase of a cell cycle. According to the manufacturer's protocol, the cells were fixed, denatured, and incubated with anti-BrdU primary antibody, secondary antibody, and substrate. The absorbance was read at 450 nm with 590 nm background subtraction with appropriate blanks.

Anti-BrdU fluorescence assay was also performed. MCF-7 cells were plated on the 96-well plate at a 5×10^3 cells/mL density. On the

following day, the cells were treated with UA 40 μM , 27 HC 1 μM , and the combination of both and incubated for 72 h. The cells were pulsed with 10 μM diluted BrdU (10 μM) in each well and incubated for 3 h prior to the assay. After 72 h of treatment, the cells were fixed using 4% PFA and incubated for 30 min at RT, followed by permeabilization using 0.4% triton for 20 min. After wash, the cells were blocked by 1% PBST followed by treatment with 2 N HCL for 1 h and further with 0.1 M boric acid for 10 min at RT. The cells were incubated with anti-BrdU antibody (BD pharmingen, 558599) and incubated at 4°C for overnight. The cells were counter-stained with Hoechst 33342 and analyzed by using Zeiss LSM980 laser scanning confocal microscope.

2.6 | Molecular docking

2.6.1 | Ligand protein preparation

Molecular docking of UA and UB was performed with ER α . Two ER α ligand-binding domains (LBD) 3ERT, ER α -LBD in complex with 4-hydroxytamoxifen (OHT), an active tamoxifen metabolite 1GWR human ER α -LBD in complex with E2, were selected. Protein structures of estrogen α (PDB: 1GWR and 3ERT) were prepared by adding hydrogen atoms and fixing the missing side chains and optimized through the Protein Preparation Wizard in the Schrödinger Suite. The LigPrep module was used to create the 3D structures of UA and UB to perform the geometric optimization. The energy minimization and optimization were performed with the OPLS force field. The grid-enclosing box was centered on the ligands complexed with the receptors and defined to surround residues positioned within 10 Å, and a scaling factor of 1.0 was set to van der Waals (VDM) radii of those receptor atoms with the partial atomic charge less than 0.25. In the docking process, extra-precision (XP) docking was utilized to generate the minimized pose of the ligands using the glide scoring function.

2.6.2 | Ligand docking

UA and UB were docked with the 3D structure of ER α with the help of GLIDE. The finest fit compounds were defined for each target by thermodynamic optimal energy value, types of interactions, the potential of bonding, and conformations. The GLIDE module of the XP visualizer analyzed the specific ligand-protein interactions. The affinity of the ligands toward the target proteins was ascertained in terms of negative glide score (kcal/mol), which is an indirect measure of binding free energy of the ligand-receptor interaction. The more negative the glide score, the stronger the interaction is.

2.7 | Estrogen receptor-alpha competitive binding assay

According to the manufacturer's instructions, the Estrogen displacement was assessed with the LanthaScreen TR-FRET ER Alpha

Coactivator Assay kit (A15887; Life Technologies). The compounds were tested in the range of 0.05–100 μ M in the presence of recommended concentrations of Fluormone™ ES2 Green (Final Concentration 3 nM), glutathione S-transferase (GST)-tagged ER-LBD (7.25 nM), and terbium (Tb)-labeled anti-GST antibody (2 nM). The plate was incubated at RT for 3 h, and time-resolved fluorescence resonance energy transfer (TR-FRET) was analyzed on a Varioskan Lux reader (thermoscientific) with the settings at 340-nm excitation and 495 and 520-nm emission. The emission ratio (520:495) was analyzed and plotted using GraphPad Prism.

2.8 | Luciferase reporter assay

Cells were plated at a density of 5×10^5 cells in 12 well plates for 24 h. The cells were further transfected with 4 μ g reporter gene 3X ERE TATA Luc (3xERE-luciferase) and 3 μ g of ER α plasmid (pHE-GO-ER) construct along with control pRL-CMV Renilla luciferase normalization vector and by Lipofectamine 3000 reagent (Invitrogen, Japan) according to the manufacturer's protocol. The transfected cells were treated with varying concentrations of UA (1–50 μ M), 27-hydroxycholesterol (1 μ M), estrogen (10 nM), and fulvestrant (1 μ M). After 18 h, the proteins were extracted, and firefly and renilla luciferase activity were measured on a TD20/20 luminometer (Turner Designs, Sunnyvale, CA) using a Dual-Luciferase Assay kit (Promega, Madison, WI E1910) according to the manufacturer's instructions. Firefly luciferase activity was normalized to Renilla luciferase expression. Each assay was performed in triplicate and repeated at least three times. 3X ERE TATA luc was a gift from Donald McDonnell (Addgene plasmid# 11354; <http://n2t.net/addgene:11354>; RRID: Addgene_11354).

2.9 | The ligand-dependent intramolecular-folding-assisted complementation study using ER-LBD intramolecular folding sensor

The cells were seeded in 12-well plates and transfected at 80% confluency using Lipofectamine 3000 (Invitrogen lot# 1810837). For transient transfection, 200 ng of pcDNA-N-RLUC-hER281-549-CRLUC, a kind gift by Dr. Ramasamy Paul Murugan, was used per well. The experiment was performed as per the previous protocol (Paulmurugan et al., 2006). A total of 10 ng of FLUC plasmid DNA per well was cotransfected to normalize for transfection efficiency. After 6 h of transfection, the cells were treated with varying concentrations of UA (1–50 μ M), 27-hydroxycholesterol (1 μ M), estrogen (10 nM), and fulvestrant (1 μ M). The cells were treated for 24 h. The luminometry assay for RLUC activity was performed. In brief, the cells were lysed in 200 μ L of $1 \times$ passive lysis buffer (Promega) on a shaking platform for 15 min at RT. The cell lysates were centrifuged for 5 min at 12,000 rpm at 4°C to remove cell debris. A total of 20 μ L of cleared supernatants was assayed for RLUC activity by the addition of 1 μ g of substrate coelenterazine h

(CAT# 301-500, Prolume) in 100 μ L of 0.05 M sodium phosphate buffer (pH 7.0) followed by photon counting in the luminometer (model T 20/20; Turner Designs, Sunnyvale, CA) for 10 s. The FLUC activity was normalized by luminometer assay using 100 μ L of the LARII substrate from Promega.

2.10 | Gene expression studies by using real-time PCR

Total RNA was isolated with Trizol reagent (Invitrogen, Carlsbad, CA) and converted to first-strand cDNA using a kit from Takara. The AB-Biosystems Cyclor Real-time PCR System was used to amplify and quantitate levels of target gene cDNA. qRT-PCR was performed with 1 μ L cDNA, 0.5 μ M specific primers (Table 1), Trefoil factor (pS2), Estrogen Receptor alpha (ER α), and progesterone receptor (PR) using TAKARA SYBR Green Kit Cat# RR820A.

2.11 | Western blot

Cells were seeded at a cell density of 1×10^6 cells in 100 mm dishes. The cells attained their morphology and were treated with the required drugs at relevant concentrations. The cells were scraped and lysed using RIPA buffer (50 mM Tris-HCl (pH 6.8), 0.1% sodium dodecyl sulfate (SDS), 0.5% NP40, 150 mM NaCl, and 0.5% sodium deoxycholate). Bradford's assay was used to quantify protein concentration. Then, 40–60 μ g of protein were loaded onto 10% gel and subjected to SDS PAGE electrophoresis. Proteins were further transferred to polyvinylidene difluoride (PVDF) membrane by western blot. The membranes were blocked with 5% BSA for 1 h and washed with TBST. The blot was incubated with primary antibody overnight at 4°C. After incubation, the blots were washed with $1 \times$ TBST. The membranes were further incubated with a suitable secondary antibody for 90 min. After washing the membrane, the respective bands were identified with the help of the Enhanced Chemiluminescence

TABLE 1 List of primers.

Sl. no.	Gene	Primer sequence (5' to 3')
1	ER α	F:ATGAAAGGTGGAACCAGGGAA R:AAGTGGCTTTTGGTCCGCTC
2	PS2	F:TTTGGAGCAGAGAGGAGGCAATGG R:TGGTATTAGGATAGAAGCACCAGGG'
3	PR	F:CGCGCTCTACCCTGCACTC R:TGAATCCGGCCTCAGGTA
4	PCNA	F:ATGCCGTCGGGTGAATTTG R:TCTCCAATGTGGCTAAGGTCTC
5	C-MYC	F:CCTCAACGTTAGCTTACCAAC R:CTGCTGGTAGAAGTTCTCCTC
6	GAPDH	F:TGCACCACCAACTGCTTAGC R:GGCATGGACTGTGGTCATGAG

(ECL) reagent (Biorad, Clarity Western ECL Substrate, #1705061). The antibodies used include ER α (F-10), Santa-Cruz, SC-8002, pS2 (Santa-Cruz, SC-271464), Progesterone Receptor (PR) (Abcam, 32085), and Gapdh (Santa-Cruz, SC-47724).

2.12 | Immunocytochemistry

For immunocytochemistry, cells plated on glass coverslips were fixed in a solution of 4% paraformaldehyde and blocked with 5% BSA and 0.3% Triton X. Cells were permeabilized with 0.3% Triton X-100. The cells were stained and incubated overnight with primary antibody ER α (1:100). After 1 \times PBS wash; cells were stained with Anti-Mouse secondary antibody, Alexa-Fluor 598 anti-rabbit, for 45 min. This was followed by DAPI (2 μ g/mL) staining and were mounted in 70% glycerol. Fluorescence was observed through 60 \times (1.3NA) or 100 \times (1.3NA) oil objectives on a Nikon inverted microscope.

2.13 | Hollow fiber assay

The assay was done in *Mus musculus*, NOD.CB17-PrkdcSCID/J, female mice weighing 20–28 g. The animals were procured from the institute animal research facility. The hollow fiber procedures were based on Hollingshead et al. (1995). The cells were harvested by standard trypsinization and resuspended at the desired cell density (1×10^6 cells/mL). The cell suspension was flushed into the hollow fibers; after which they were heat-sealed and cut at 2 cm intervals. The fibers were incubated in the DMEM medium in six-well plates 24 h prior to surgical implantation in immunocompetent female ovariectomized NOD-SCID mice. Ovariectomy was done 3 weeks prior to implantation. Three fibers per cell lines, namely, MCF-7, MDA-MB 231, and T47D, were implanted subcutaneously and intraperitoneally. Separate in vitro control fibers were also prepared and incubated in the DMEM medium during the experiment.

2.14 | Drug administration and retrieval of the cancer cells from the hollow fibers

The animals were kept in cages in an air-conditioned room with alternating light and dark cycles and had access to food and autoclaved water ad libitum. The protocol was approved by the Institute Animal Ethical Committee (IAEC/566/SREJ/2016, IAEC/767/SREJ/2019). The mice were treated on Day 3 with different oral administrations. There were six experimental groups viz.: (1) Vehicle control (DMSO control); (2) UA (50 mg/kg/bw); (3) UA (40 mg/kg/bw); (4) 27-HC (10 mg/kg/bw); (5) UA (40 mg/kg/bw) and 27-HC (10 mg/kg/bw); (6) UA (50 mg/kg/bw) and 27-HC (10 mg/kg/bw); and (7) E2 (1 mg/kg/bw). The mice were sacrificed by CO₂ inhalation on Day 5, and the fibers were excised. Excess host tissue was removed, the fibers were transferred into prewarmed DMEM medium and incubated for at least 1 h, and MTT assay was done.

2.15 | Assessment of cytotoxicity

Prewarmed DMEM (1.5 mL) containing 1 mg MTT/mL was added to each well. After 4 h incubation at 37°C in a 5% CO₂ humidified atmosphere, the culture medium was aspirated, and the fibers were washed with normal saline containing 2.5% protamine sulfate (w/v). The fibers were stored overnight at 4°C. The solution was aspirated, and the samples were rewashed for 4 h at 4°C. Each fiber was wiped with gauze to remove stained debris on the outside of the fiber and transferred to 24-well plates (1 fiber/well). The fibers were cut in half and allowed to dry overnight at RT. The produced formazan crystals were dissolved in dimethylsulphoxide (DMSO; 250 μ L well) and incubated for 4 h at RT on a rotating platform while protected from the light. Aliquots of 150 μ L of extracted solution were transferred to individual wells in 96-well plates. Absorbance (OD) was measured at 550 nm using a spectrophotometer (Biorad). Net cell growth was calculated using the formula ((mean OD_{day10} – mean OD_{day0})/(mean OD_{day0}) \times 100%.

2.16 | Biochemical analysis

After retrieving fibers, the blood samples were collected by cardiac puncture. The blood samples were left at RT and centrifuged at 10,000 rpm for 10 min. The serum samples were then analyzed for Total Cholesterol, Triglyceride, AST/GOT, Alkaline Phosphatase, GPT/ALT, Total Bilirubin, Albumin, Total Protein, Calcium, Blood urea, and nitrogen.

2.17 | Uterine histopathology study

The uterine wet weights and epithelial heights were the primary physiological endpoints utilized to assess estrogenicity. Uterine wet weights were measured. Sections of the uterus were stained with hematoxylin and eosin and prepared for light microscopy. The harvested uterus was preserved in 10% buffered formalin and embedded in paraffin wax sectioned (4 μ m) and stained for histopathological evaluation using eosin and hematoxylin staining. The histopathological evaluation in this study was performed using a light microscope. The height of the luminal epithelium (\times 20 objective) was determined using optical micrometry. Measurements were standardized using the image of a stage micrometer at the same magnification.

2.18 | Statistical analysis

Results were expressed as a mean \pm standard deviation of three biological replicates. *p* value was determined using paired two-sided Student's *t*-test, one-way ANOVA, or two-way ANOVA, depending on the experiments. *p* values were considered significant at *****p* < 0.0001; ****p* < 0.001; ***p* < 0.01; **p* < 0.05.

3 | RESULTS

3.1 | Screening of cell viability in breast cancer cells with UA and UB treatment

The evaluation of cell viability was performed by the MTT assay on two ER-positive cancer cell lines, MCF-7 and T47D, as well as a non-tumorigenic epithelial cell line, MCF-10A. The cells were treated with different concentrations (1–100 μM) of UA and UB for 5 days (Figure 1a,b). Our results indicated that UA treatment induced a more significant reduction in cell viability compared with UB treatment in both the MCF-7 and T47D cell lines, while no significant effect was observed on the MCF-10A cell line (Figure 1d). Notably, at a concentration of 40 μM , UA inhibited 27-HC mediated cell proliferation from 117% to approximately 57%, while UB reduced it to around 75%, as

evident in Figure 1c. There was no notable impact on cell viability compared with the control ($n = 6$, 100 ± 0.01) with the usage of 0.01% DMSO as the vehicle.

The mitochondrial membrane potential Ψ_{mito} was measured by (TMRM) fluorescent staining. We observed that the mitochondrial membrane potential was perturbed upon UA and UB treatment, indicating apoptosis. However, UA induced mitochondrial membrane permeability and membrane depolarization to a greater extent (50%) compared with UB (21%), implying a higher level of apoptosis (Figure 2a). These findings were in line with the MTT assay results. Further, the cells were treated with varying concentrations of UA, namely, 25, 40, and 50 μM . Among these, UA at 50 μM showed the highest population of cells (51%) with reduced TMRM, while 27-HC failed to induce any mitochondrial membrane loss (Figure 2b,c). UA at different concentrations could trigger a loss of membrane potential

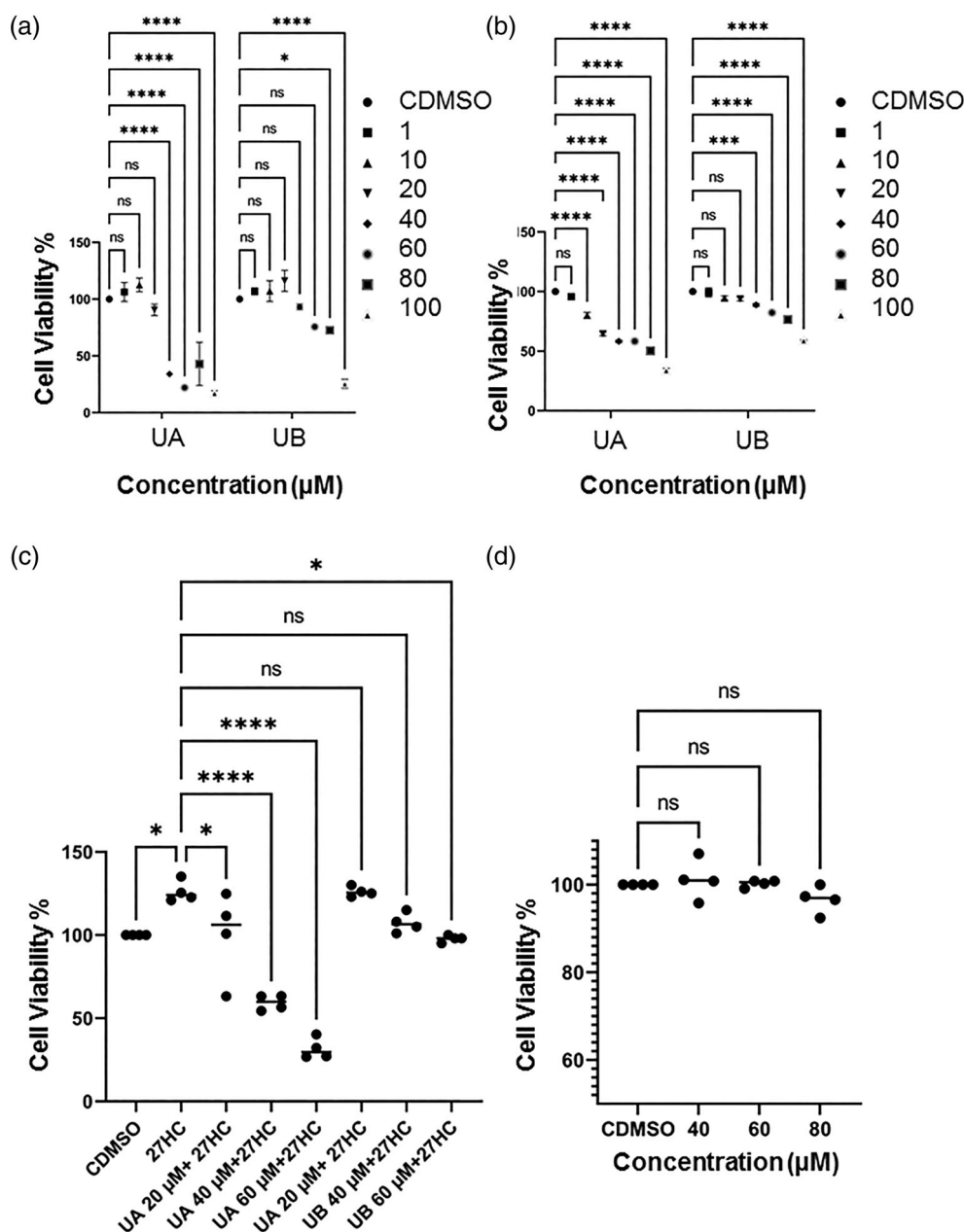


FIGURE 1 MTT assay was used to determine viability of breast cancer cells treated with different test compounds. (a) MCF-7 Cells were treated with UA or UB at different concentrations from 1 μM to 100 μM and cell viability was calculated after 5 days. (b) T47D Cells were treated with UA or UB at different concentrations from 1 μM to 100 μM and cell viability was calculated after 5 days. (c) MCF-7 cells were treated with UA or UB in combination with 27-HC (1 μM) or 27-HC alone. (d) MCF-10A cells which is normal mammary epithelial cell line were treated with 40–80 μM UA and as evident in MTT assay, there was no significant toxicity in normal cell lines. The graphs are represented as mean \pm SD, $n = 3$ replicates. p value was determined using two-way ANOVA. p values were considered significant at *** $p < 0.0001$; ** $p < 0.001$; * $p < 0.01$, * $p < 0.01$.

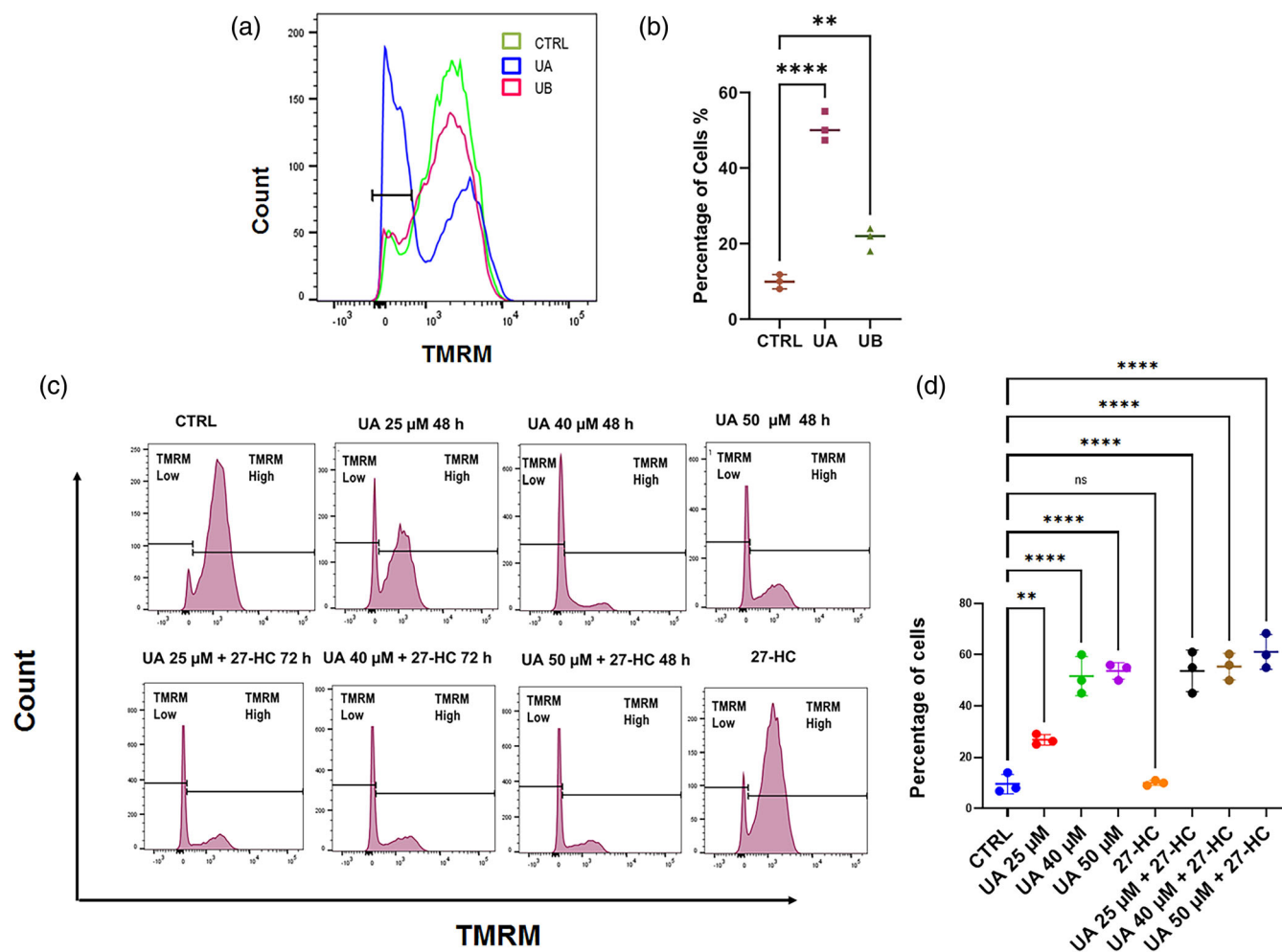


FIGURE 2 Characterization of tetramethylrhodamine methyl ester (TMRM)-low and TMRM-high cell populations by fluorescent activated cell sorting (FACS) analysis in MCF-cells upon exposure to varying test compounds. (a) The figure shows overlapping representative histogram of $\Delta\Psi_m$ by TMRM vehicle control (0.1%DMSO), UA (40 μ M) and UB (40 μ M) treated cells. (b) The graph representing mean fluorescence intensity \pm SD of TMRM in the apoptotic population/low Ψ_m in each treatment. (c) Cells treated with vehicle control (0.1% DMSO), UA (25, 40, and 50 μ M) treated cells. (c) UA (25, 40, and 50 μ M) in combination with 27-HC (1 μ M) cells and 27-HC (1 μ M) alone. (d) The graphs show mean fluorescence intensity \pm SD of TMRM in the apoptotic population/low Ψ_m in each treatment. Density plots and histograms represent $n = 3$ replicates. p value was determined using paired one-way ANOVA. p values were considered significant at **** $p < 0.0001$; *** $p < 0.001$; ** $p < 0.01$; * $p < 0.01$.

even in the presence of 27-HC (Figure 2c). Moreover, to understand the type of cell death induced by UA treatment, annexin-PI staining was performed. The results showed a significant increase in late apoptosis upon UA treatment. At a concentration of 40 μ M for 48 h, UA treatment resulted in approximately 53% late apoptosis (Q2) and nearly 5.23% early apoptosis (Q3) (Figure 3a,b). In addition, UA induced apoptosis in the 27-HC treated population by nearly 25%. We also confirmed that UA did not induce apoptosis in normal MCF-10A cells (Figure 3c,d).

3.2 | Reduction of 27-HC-induced proliferation treated with UA

In light of the higher antiproliferative activity demonstrated by UA, additional experiments were conducted using this compound. To

further assess its antiproliferative activity, BrdU assay was performed using both an anti-BrdU fluorescence assay and a Horseradish peroxidase (HRP) based assay. BrdU, a thymidine analog, is incorporated into the cell genome during replication, reflecting the extent of cell division and proliferation. The anti-BrdU fluorescence assay clearly showed that treatment with UA (40 μ M) alone and in combination with 27-HC significantly reduced BrdU incorporation compared to control and 27-HC treated cells (Figure 4a). The quantitative evaluation of BrdU incorporation using the HRP-based method showed that UA (40 μ M) reduced cell proliferation to 0.6 (approximately 40%) compared to the control (Figure 4b). Furthermore, UA inhibited the 27-HC-induced cell proliferation by 67% when compared to 27-HC treated cells (Figure 4b). The expression of proliferating cell nuclear antigen (PCNA) and c-Myc were assessed following UA treatment. PCNA is a useful marker for assessing cell proliferation and prognosis in breast cancer when used in conjunction with other breast cancer

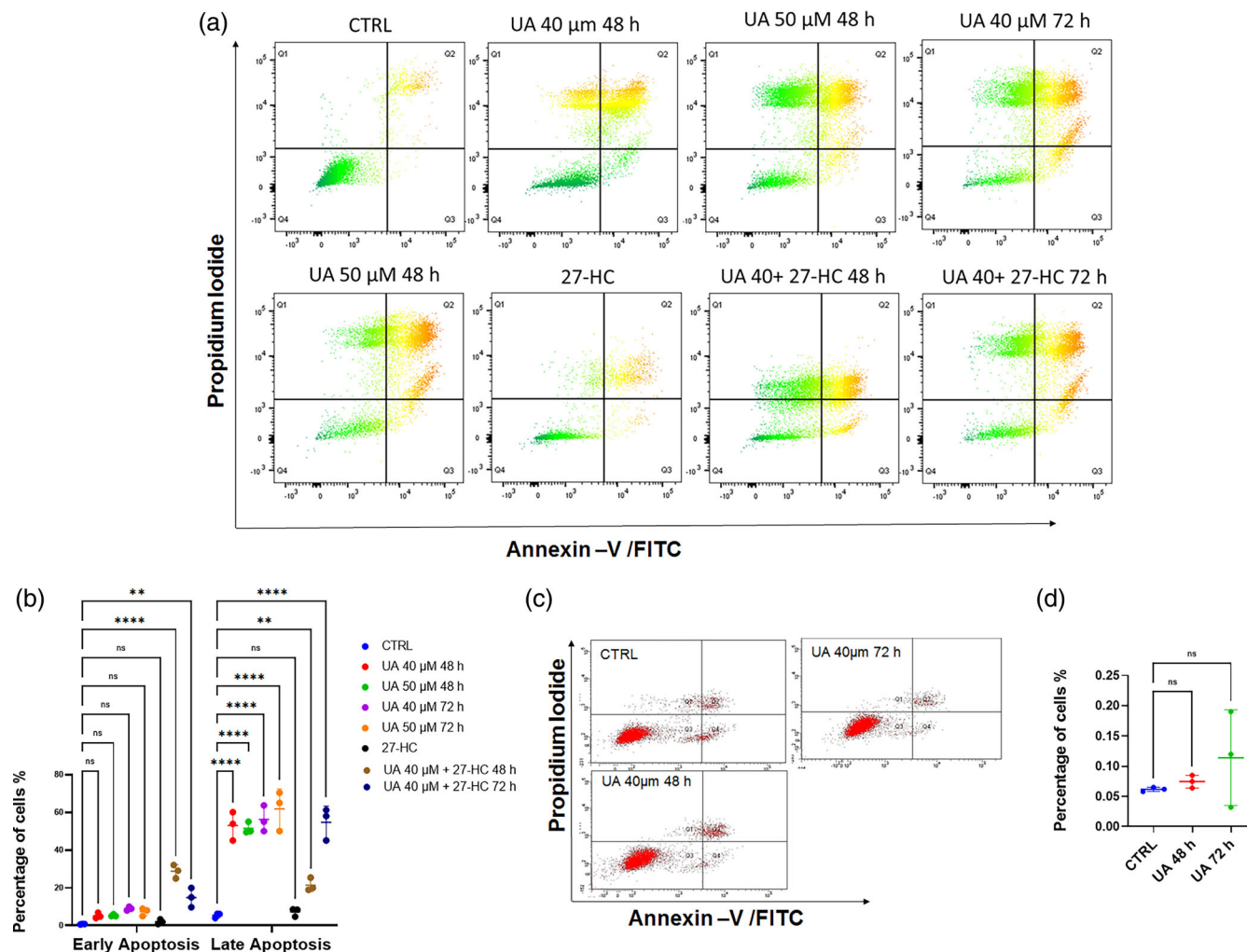


FIGURE 3 Detection of apoptosis by annexin V-FITC/propidium iodide dual staining. A. MCF-7 cells were treated with varying concentrations of test compounds. (a) Representative density plot which treated with vehicle control (0.1% DMSO), UA 40 μM, 50 μM for 48 h and 72 h, 27-HC alone (1 μM) or 27-HC in combination with UA 40 μM for 48 and 72 h. (b) The mean percentage representation of cells in early apoptosis (Q3) and late apoptosis (Q2) shown in (a) as determined by flow cytometry with. (c) MCF-10A cells were treated with UA 40 μM. (d) The mean percentage of cells in early apoptosis (Q3) and late apoptosis shown in (d) as determined by flow cytometry. In each density plot, quadrant Q1 shows necrotic cells (annexin- PI+); Q2 late apoptotic cells (annexin+ PI+); Q3 early apoptotic cells (annexin+ PI-), and Q4 viable cells (annexin- PI-). The experiments have been done in biological triplicates, $n = 3$ replicates. The data represent \pm SD. p value was determined using two-way ANOVA. p values were considered significant at **** $p < 0.0001$; *** $p < 0.001$; ** $p < 0.01$; * $p < 0.01$.

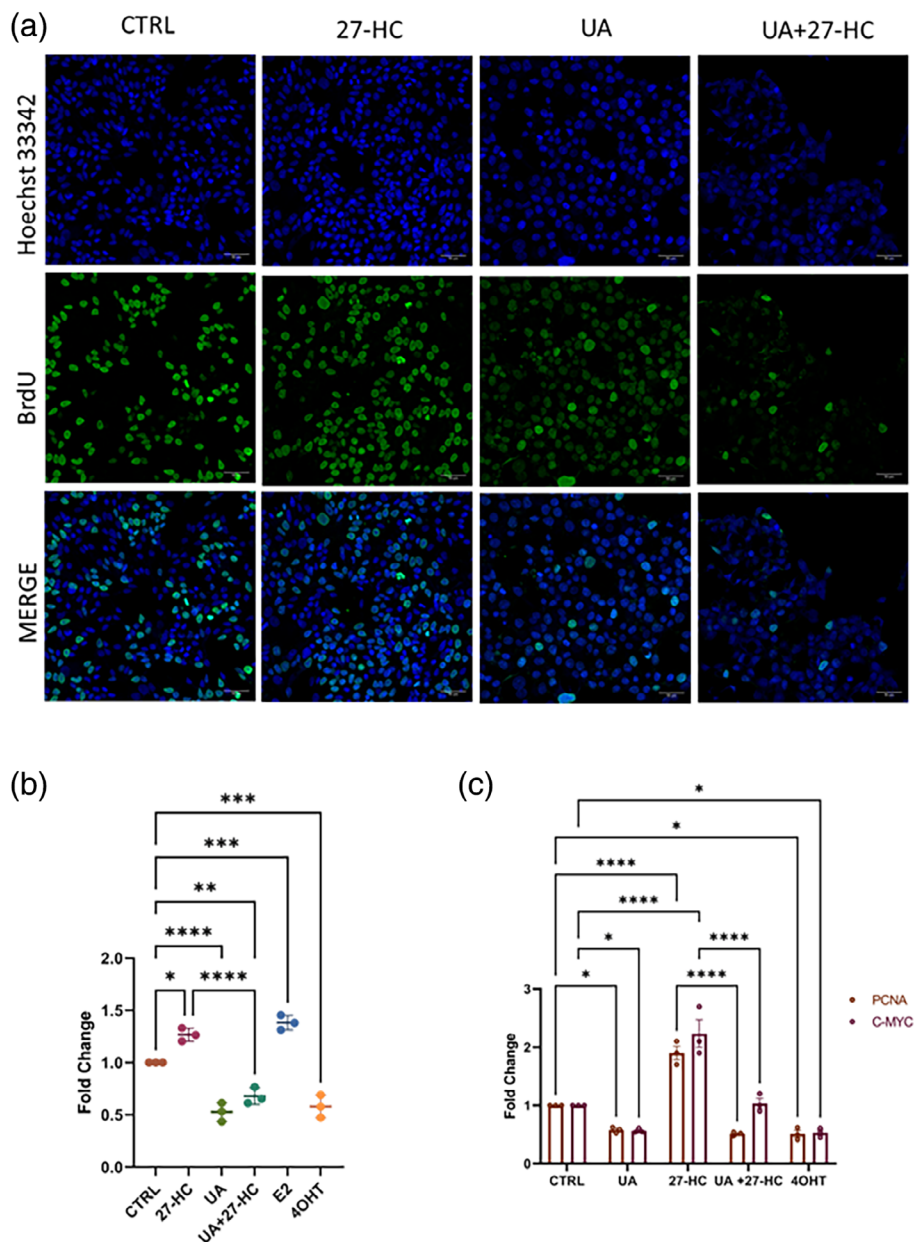
markers such as ER, progesterone receptor (PR), and human epidermal growth factor receptor 2 (HER2) (Jurikova et al., 2016; Ma et al., 2021). On the other hand, c-Myc, an estrogen-responsive gene, is closely associated with the prevalence of breast cancer (Chen et al., 2020; Gao et al., 2023; Lee et al., 2019). The expression of both PCNA and c-Myc was reduced upon UA treatment, further confirming its ability to reduce proliferative activity (Figure 4c).

3.3 | Molecular modeling indicating binding of UA and UB to ER α

Next, to understand the reason behind the superior activity of UA over UB, we conducted docking studies with both compounds on the

agonist conformation 1GWR and antagonist conformation 3ERT of ER α (Figure 5a-h). Our results showed that UA had a slightly higher affinity to 1GWR than 3ERT, while UB had a lower affinity to 1GWR than 3ERT (Table 2). In addition, UA demonstrated a higher affinity towards 1GWR than UB. Further analysis revealed that the hydroxyl groups of UA formed hydrogen bonds with HIE 524 and LEU 387 when docked with the agonist conformation 1GWR. The results showed that most interactions between ligands and ER α were hydrophobic. The hydrophobic core of ER α extensively interacted with hydrophobic residues in the ligand-binding pocket, and the presence of hydrophobic substituents with varying sizes and shapes at various positions could enhance the binding affinity (Lee & Barron, 2017). In contrast, UB formed π - π stacking with PHE404 in addition to the hydrogen bonds with GLU353 when docked with 1GWR. Besides, UA

FIGURE 4 Detection of Cell proliferation: (a) BrdU assay was carried out after cells treating with compounds for 72 h. The incorporated BrdU was stained with anti-BrdU Alexa Fluor®488 monoclonal antibody (green color) with cell nuclei counter-stained with Hoechst 33342 (blue color). Cells were treated with vehicle control (0.1%DMSO) or UA (40 μ M) treated cells. (b) BrdU Proliferation Assay: cells were treated with UA at 40 μ M individually and in combination with 27-HC (1 μ M) or 27-HC alone. The graphs are represented as mean fold change with respect to control \pm SD, $n = 3$ replicates. p value was determined using an paired two-sided Student's t -test. (** $p < 0.001$; ** $p < 0.01$; * $p < 0.01$). The bar graph represents the qRT-PCR analysis for PCNA and has revealed the downregulation of its expression in different treatments, UA (40 μ M), 27-HC (1 μ M), and combination (UA 40 μ M + 27-HC 1 μ M), treated cells. The GAPDH was used as normalization control and the error bar represents the standard deviation of three independent replicates. The data represent \pm SD, $n = 3$. p value was determined using paired two-way ANOVA. p values were considered significant at *** $p < 0.0001$; *** $p < 0.001$; ** $p < 0.01$; * $p < 0.01$.



and UB formed hydrogen bonds with ARG 394 and GLU353 when docked with antagonistic 3ERT conformation.

3.4 | UA exhibiting ER modulatory activity

In order to assess whether UA can activate estrogen response elements (EREs), we evaluated its ability to induce luciferase transcription since the classical model of ER activation involves binding to EREs. The results showed that UA induced luciferase transcription (Figure 6a). Further, MCF-7 cells were treated with various concentrations of UA, and the outcomes implied a significant increase in luciferase expression at all the concentrations tested (1–50 μ M) but lower than the positive controls, E2 and 27-HC. However, when UA in combination with 27-HC was used at higher

concentrations (40–50 μ M), there was a decrease in the ERE-luciferase activity compared with cells treated with 27-HC alone. The ER α antagonist-specific intramolecular-folding sensor was utilized to evaluate RLUC complementation, and the results showed significant RLUC complementation in transfected cells exposed to UA and 4-hydroxytamoxifen (4-OHT), an active metabolite of tamoxifen, in comparison with carrier control cells (Figure 6b). It was observed that UA, at concentrations ranging from 1 to 50 μ M, induced RLUC complementation to a degree comparable with that of 4-OHT and higher than that of estrogen. This indicated that UA binding led to SERM-bound ER α conformation. Using the LanthaScreen TR-FRET competitive binding assay, we found that UA exhibited binding affinity to ER α with an EC₅₀ of 5.14 μ M (Figure 6c). These findings offer supporting evidence that UA can effectively bind to ER α .

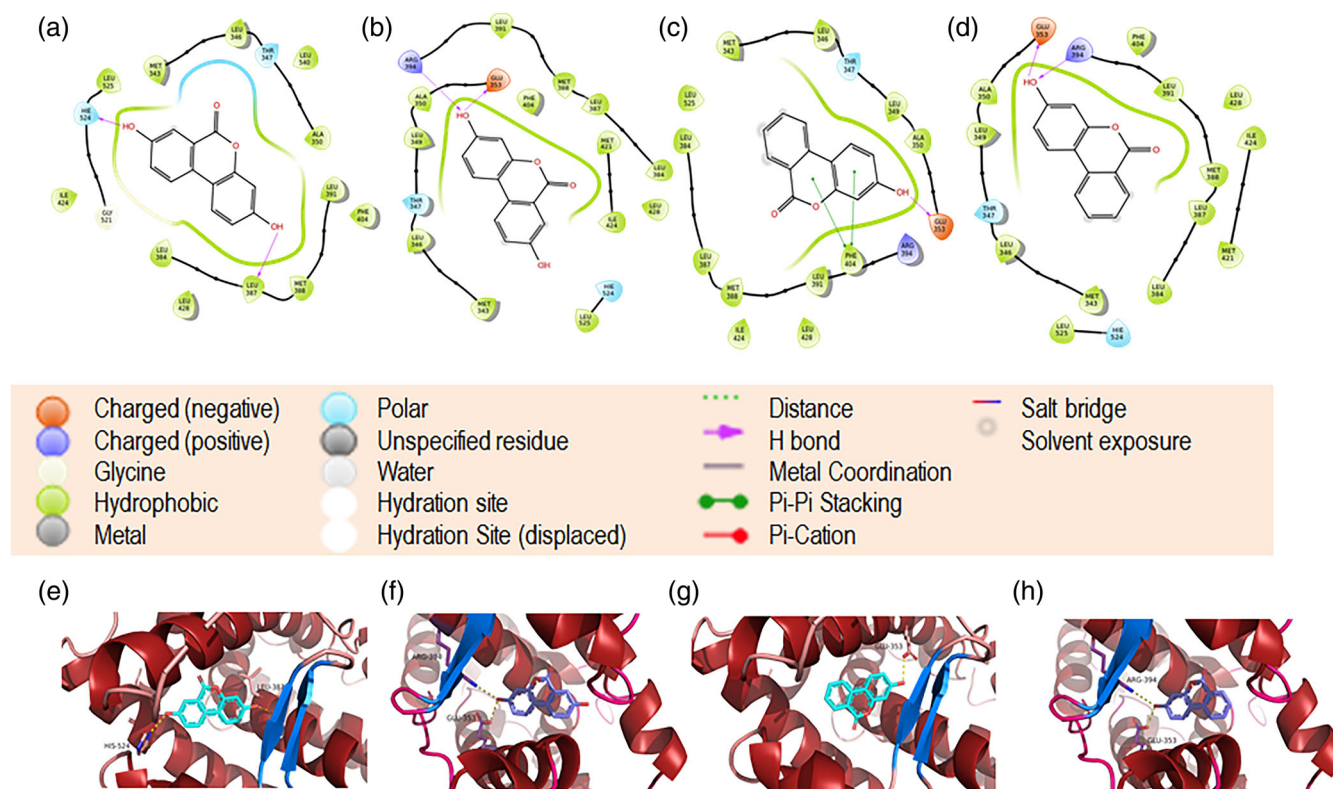


FIGURE 5 Docking of UA and UB with ER α -LBD receptors. (a and b) 1D representation of the interactions between UA with 1GWR, the agonist conformation and 3ERT, antagonist conformation in best docked pose and (e and f) their respective 3D representations (c). (c and d) 1D representation of the interactions between UA with 1GWR, the agonist conformation and 3ERT, antagonist conformation in best docked pose while (g and h) are their respective 3D representations.

TABLE 2 UA and UB were docked with different conformations of ER α 1GWR (agonist conformation) and 3ERT (antagonist conformation) using GLIDE.

Protein	Ligand	XP GScore	Glide gscore	Glide evdw	Glide ecol	Glide energy	Gliden einternal	Glide emodel XP	HBond
1GWR	Urolithin A	-9.317	-9.317	32.142	-5.726	-37.868	-1.334	-52.413	-0.597
1GWR	Urolithin B	-8.209	-8.209	-30.025	-7.496	-37.521	0.108	-46.702	-0.637
3ERT	Urolithin A	-8.106	-8.106	-33	-7.987	40.987	0.02	-54.989	-0.637
3ERT	Urolithin B	-8.103	-8.103	-29.304	-9.838	-39.143	0.01	-49.81	-0.548

Note: The scores are represented here. XP GScore: extra-precision docking score, including all additional terms. Glide gscore: Glide Score. Glide evdw-van der Waals energy. Glide ecol: Coulomb energy. Glide energy: modified Coulomb-van der Waals interaction energy. Glide emodel: model energy, Emodel. Glide einternal: internal torsional energy. Hbond: hydrogen-bonding term in the GlideScore.

3.5 | Differential effects of UA on ER α downstream targets

This study observed that UA at varying concentrations could induce the expression of pS2, an estrogen-inducible gene containing ERE at the promoter, at both transcriptional and translational levels (Figure 7a,b). However, there was no considerable induction in PR, another estrogen-inducible gene, at transcriptional and translational levels (Figure 7b,c). Despite their opposing nature, ER ligands, including agonists, antagonists, or SERMS, have been reported to have common targets and actions (Frasor et al., 2004, Guan et al., 2019). On the contrary, ligands with similar functions that bind to ER α can

induce different ER α conformations, resulting in the activation or repression of unique genes. This phenomenon can hold true with the ligands 27-HC and UA, which show differences in response to estrogen-inducible genes. Although progesterone receptors (PR-A and PR-B) are responsive to estrogen, they do not contain palindromic EREs. Instead, they contain an ERE half-site upstream of two adjacent Sp1 sites (Petz et al., 2004). UA binding to ER α might selectively promote binding to classical ERE elements rather than Sp1 sites, which could explain the lack of significant difference in PR expression. Nonetheless, further experiments are required to elucidate the underlying mechanism. Additionally, we observed downregulation of ER α mRNA across all the treatments, including varying concentrations of

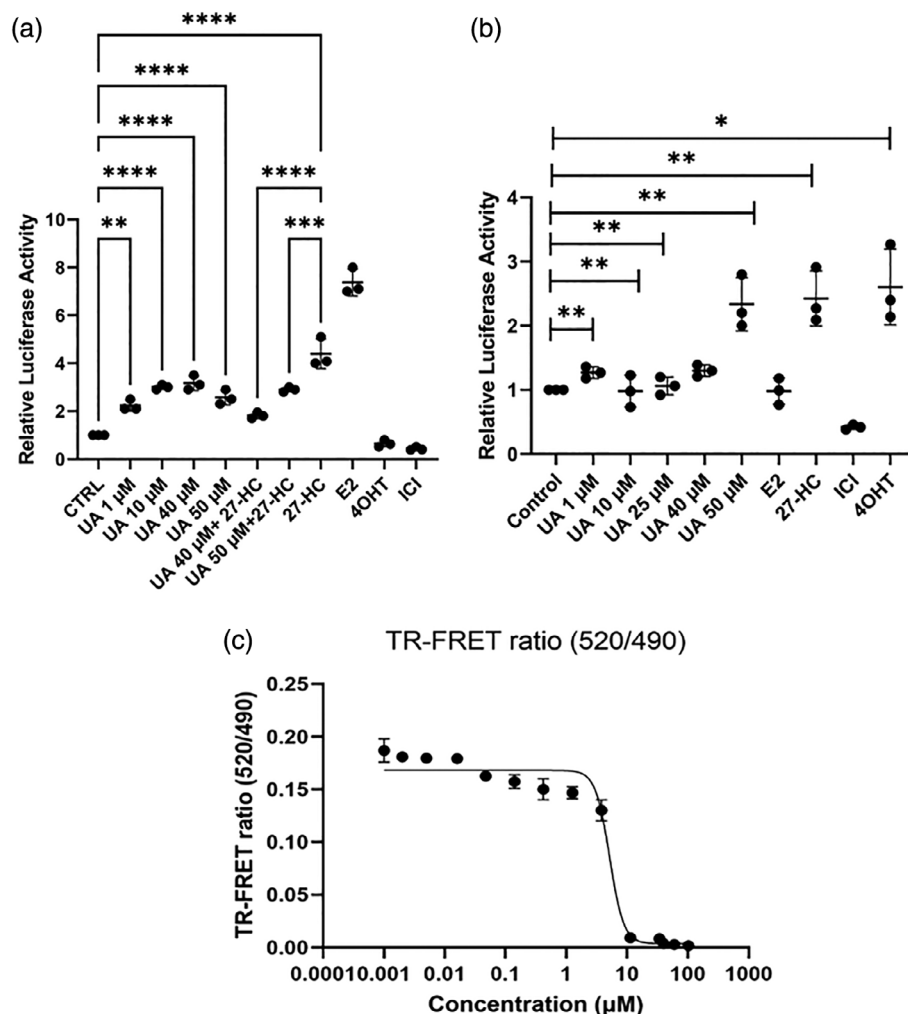


FIGURE 6 Binding affinity and specificity of UA and ER agonist/antagonist activity. (a) MCF-7 Cells were transfected with ERE-luc and *Renilla* luciferase constructs in medium containing 5% CTS. Twenty-four hours after the transfection, the cells were treated with different concentrations of UA (1–50 μ M), 4-OHT (1 μ M), E2 (1 μ M), ICI (1 μ M), and 27-HC (1 μ M) and UA in combination with 27-HC and further luciferase activity was measured, ERE-driven luciferase activity was measured and normalized to that of *Renilla* luciferase, and the activity of ER in vehicle-treated conditions is set to 1. (b) MCF-7 cells were either transfected with N-RLUC-hER281–549/G521T-C-RLUC or vector plasmid and treated with different concentrations of UA and 4-OHT (1 μ M), E2 (1 μ M), ICI (1 μ M), and 27-HC (1 μ M) or vehicle control DMSO and RLUC activity was determined 18 h after treatment by luminometer assays with cell lysates. (c) TR-FRET ER α competitive binding assay with UA. A 100 \times stock concentration of UA in 100% DMSO was diluted to 4 \times concentration (4% DMSO) in assay buffer and challenged with a control competitor, ES2. Dose–response curves (0.1–100 μ M) of UA for the displacement of ES2 from ER α measured as loss of FRET by using the time-resolved fluorescence resonance energy transfer (TR-FRET) assay. Data presented are an average of biological triplicates, $n = 3$. p value was determined using paired two-way ANOVA. p values were considered significant at *** $p < 0.0001$; ** $p < 0.001$; * $p < 0.01$; $p < 0.01$.

UA (1, 20, 40, and 50 μ M), 27-HC (1 μ M), E2 (10 nM), ICI (1 μ M), and 4-OHT (1 μ M). This is consistent with previous reports of reduced mRNA levels of ESR1 in the presence of all ligands (Kocanova et al., 2010).

3.6 | Non-degradation ER α with UA treatment

The binding of different ligands to ER α can induce various structural alterations, impacting cofactor binding and ER α stability (Guan et al., 2019). Ligands such as estrogen, 27-HC (DuSell et al., 2008), and fulvestrant (ICI) have been reported to induce ER α degradation,

with ICI causing the most rapid degradation (Guan et al., 2019). Conversely, tamoxifen is shown to stabilize ER α (Figure 8). In our study, UA did not cause any significant degradation of ER α protein, as observed in the immunoblot and immunofluorescence analyses (Figure 8a–c), which was comparable to the effect of 4-OHT, the positive control (Figure 8c).

3.7 | Hollow fiber assay

Furthermore, it was observed that UA had a greater effect on reducing cell viability in breast cancer cell lines in subcutaneous implants

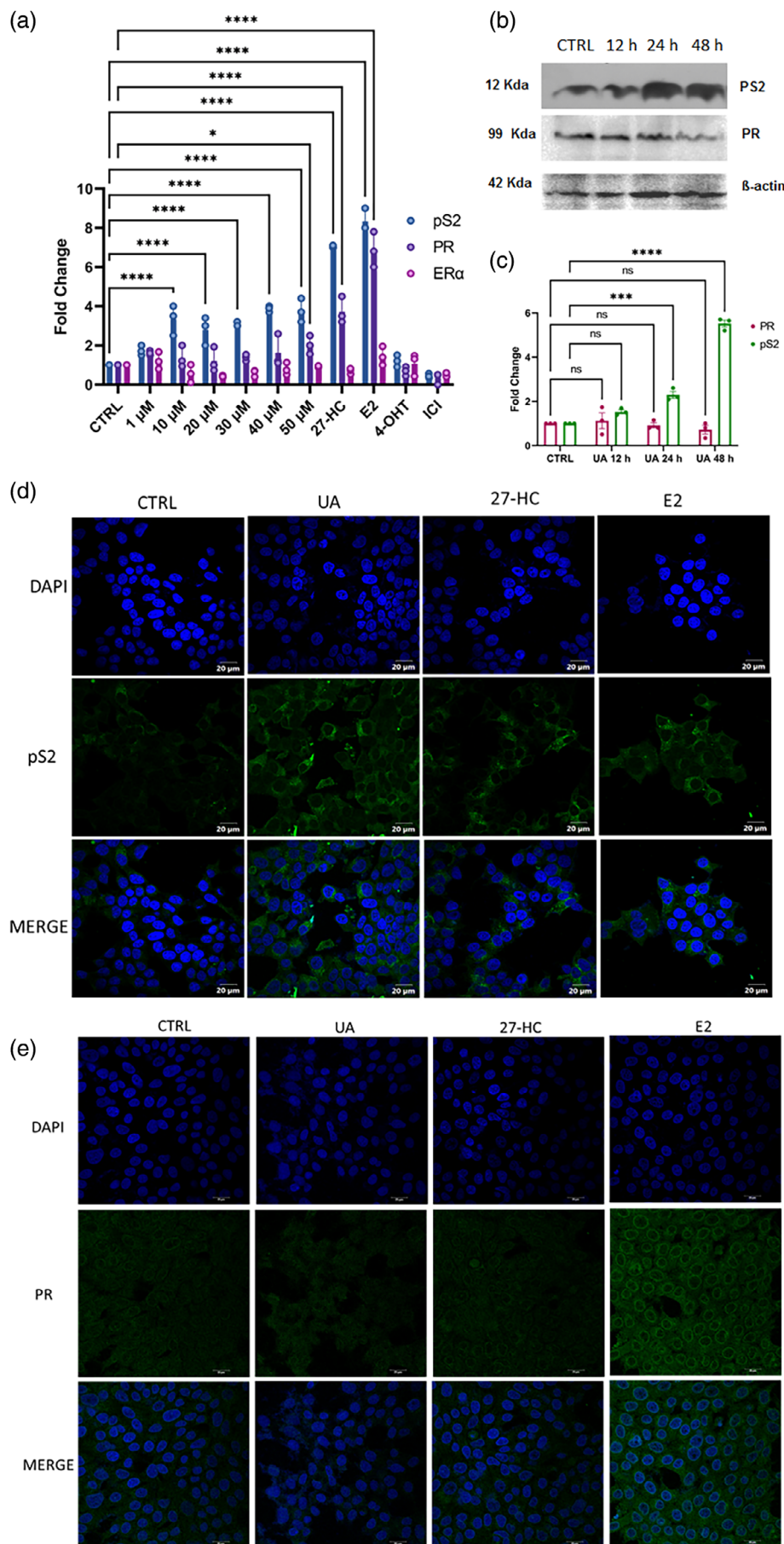
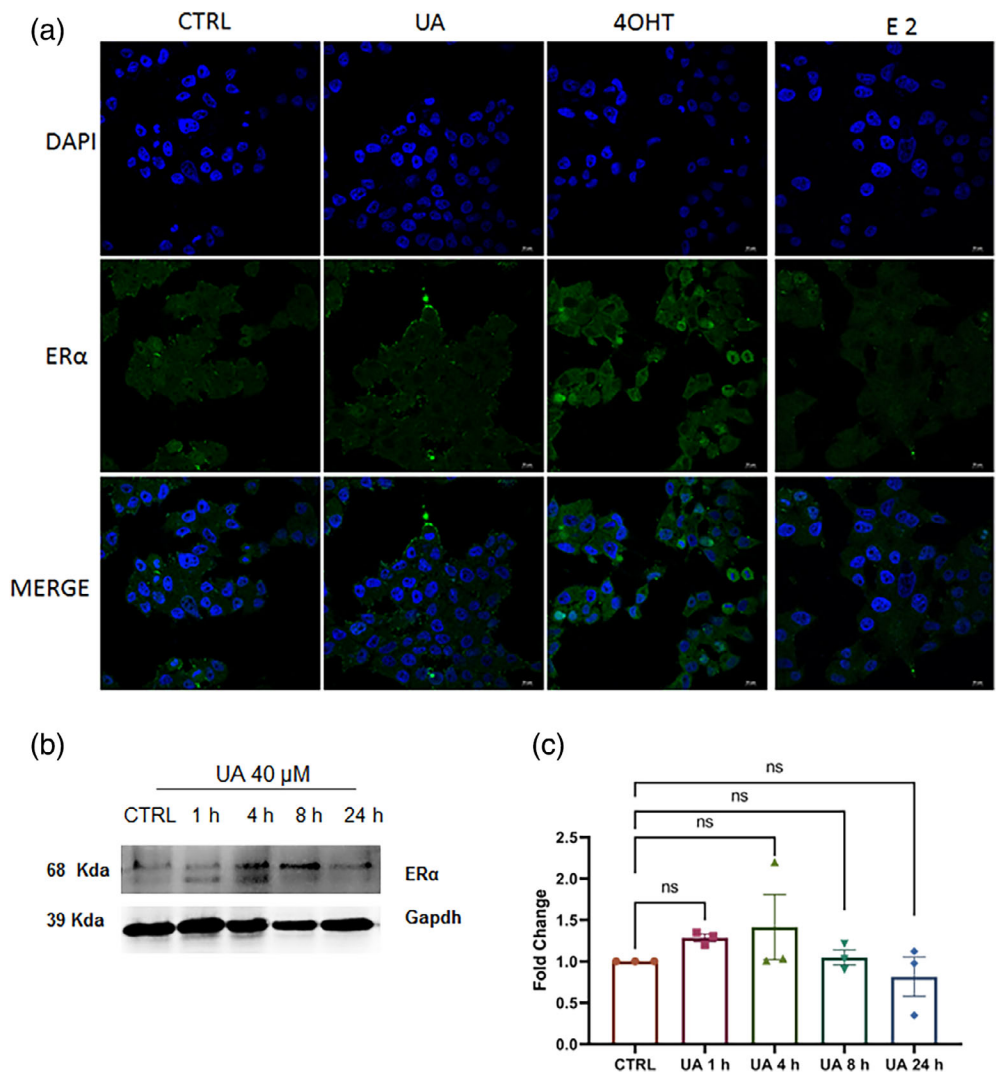


FIGURE 7 Effect of UA on ER α targets. (a) MCF-7 cells were treated with 0.1% (v/v) DMSO, or different concentrations of UA (1–50 μ M), 27-HC (1 μ M), 4-OHT (1 μ M), E2 (100 nM), or ICI (1 μ M) for 24 h. (b) The gene expression of estrogen receptor 1 (ESR1), progesterone receptor (PR), and TFF1 was assessed by real-time PCR and normalized to the expression of the housekeeping genes GAPDH. The results are expressed as the fold change in gene expression compared with that of DMSO. (c) MCF-7 cells were treated with 0.1% (v/v) DMSO, or UA (40 μ M) for 12–48 h and western blot was performed probed for pS2 (TFF1) and PR antibodies. (c) The expression of the proteins was normalized to the endogenous control β -actin. *p* values were determined using paired two-way ANOVA. Data presented are an average of biological triplicates, $n = 3$. *p* values were considered significant at *** $p < 0.0001$; ** $p < 0.001$; * $p < 0.01$, and * $p < 0.01$. (d) Immunofluorescence staining of pS2 (0.1% DMSO), UA (40 μ M), 4-OHT (1 μ M), and E2 (100 nM) for 24 h. (e) Immunofluorescence staining of PR in MCF-7 cells treated with vehicle control (0.1% DMSO), UA (40 μ M), 4-OHT (1 μ M), and E2 (100 nM) for 24 h.

FIGURE 8 Effect of urolithin A on ER α expression.

(a) Immunofluorescence images shows the expression of ER α after 4 h of treatment with vehicle control (DMSO 0.1%), or UA (40 μ M), 27-HC (1 μ M), and 4-OHT (1 μ M). There was no significant reduction in ER α upon UA treatment. (b) Cells were treated with UA (40 μ M) for 1–24 h and the whole cell lysate was subjected to immunoblotting and probed with ER α . There was no much significant difference in ER α levels upon UA treatment at any time points of treatment. (c) The protein expression of ER α was normalized with GAPDH and expressed as fold change over control. Data presented are an average of biological triplicates, $n = 3$. p values were considered significant at *** $p < 0.0001$; ** $p < 0.001$; * $p < 0.01$; and * $p < 0.01$.



than peritoneal inserts at both the doses of 40 and 50 mg/kg bw/d (Figure 9a,b). In contrast, 27-HC (1 mg/kg bw/d) induced ER-positive cell proliferation in subcutaneous and peritoneal inserts. In addition, UA reduced the 27-HC-induced cell viability in MCF-7 and T47D cells in subcutaneous and peritoneal implants, with a more pronounced effect observed in subcutaneously placed hollow fiber. This variation in response could be attributed to differences in the availability of metabolites in different tissues.

3.8 | Morphometric analysis of uterus

Further, to evaluate estrogenicity, the primary physiological measures utilized were uterine wet weights and epithelial heights (Figure 9c–e). When given at a dose of 1 mg/kg bw/d, the positive control E2 caused a three-fold increase in uterine wet weight in OVX animals compared to the vehicle-treated OVX control (Figure 9c). There was no significant difference in uterine wet weight between the groups that received UA (40 and 50 mg/kg bw/d), 27-HC (1 mg/kg bw/d), and the vehicle-treated OVX control group. However, the

combination of UA and 27-HC demonstrated an increase in uterine weight, showing slightly hormone-like activity.

In addition, the gross morphology of the uterus appeared normal in the vehicle-treated control group. E2 treatment presented a substantial increase in the epithelial thickness of the uterus compared to the vehicle-treated OVX control mice. Besides, UA (50 mg/kg bw/d) treatment showed a disordered proliferative endometrium with increased thickness and more cystic glands, possibly due to the unopposed action of estrogen (Figure 9d). 27-HC treatment also resulted in a proliferative endometrium with no change in the thickness of the epithelial uterine compared with the control. Meanwhile, the combination treatment (40 mg/kg bw UA+ 27-HC) showed secretory endometrium with increased thickness and more coiled glands. On the other hand, treatment at higher concentration (50 mg/kg bw UA + 1 mg/kg bw 27-HC) showed disordered proliferative endometrium, suggesting that UA or 27-HC can induce a partial persistent estrogen-like effect when administered either separately or in combination. As expected, the mice group treated with estrogen as the positive control exhibited hyperplastic hypersecretory endometrium with increased thickness, providing clear evidence of a hormonal effect (Figure 9d,e).

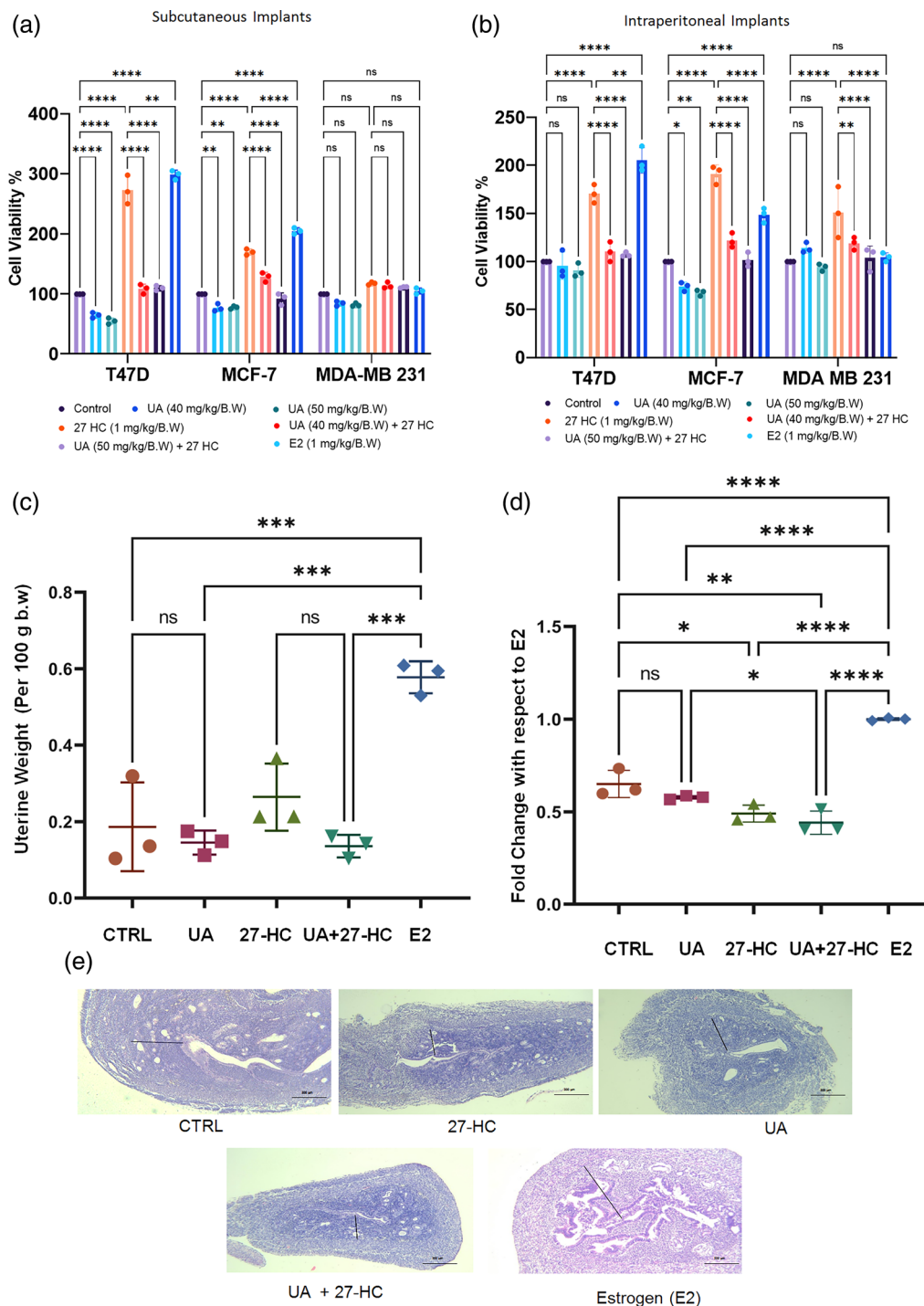


FIGURE 9 Antitumor action of UA on using in vivo Hollow Fibre Assay (HFA) and assessment of uterine morphology. The tumor cell lines T47D, MCF-7, and MDA-MB 231 were grown in hollow fibres at a density of 1×10^6 cells/mL. The fibers were incubated for 24 h at (37°C) and implanted into OVX-SCID mice. The mice were treated with different compounds as indicated for 5 days and were retrieved. The cell growth was assessed using MTT assay as described in materials and methods. The percentage of cell growth is presented here. (a) In subcutaneous implants. (b) Intraperitoneal implants. (c) Average uterine weight relative to total body weight. The endometrial thickness of each treatment group was compared with positive control estrogen, 17- β -estradiol (E2), and fold change was calculated. Endometrial thickening and uterine weight in the other treatments were lower when compared to E2. All values are means \pm SE. Compared to OVX control, * $p < 0.05$; ** $p < 0.01$; *** $p < 0.001$; **** $p < 0.0001$. (e) Representative photomicrographs of uterine hematoxylin and eosin-stained sections in ovariectomized (OVX) mice. The treatment groups: (a) control group untreated OVX mice; 27-HC (10 mg/kg bw), UA (50 mg/kg bw), and UA + 27-HC, E2 (1 mg/kg bw). The line indicates the endometrial thickness. The image was taken in 20 \times objective; bar = 100 μ m.

Hence, it can be confirmed that UA elicits a hormonal response but does not induce hyperplasia similar to estrogen. However, it would be necessary to use better rodent models, such as Sprague–Dawley rats, and extend the treatment duration to obtain confirmation since SCID mice produce minimal inflammatory responses.

3.9 | Evaluation of biochemical blood parameters

Next, various blood parameters, such as total cholesterol, triglyceride, aspartate aminotransferase, alanine aminotransferase, alkaline phosphatase, total bilirubin, albumin, total protein, calcium, blood urea, and nitrogen were measured to evaluate lipid profile, liver function, and kidney function. All parameters were found to be within the normal range. Notable, UA treatment did not cause any abnormal changes in the blood biochemical parameters, and all parameters in the treatment groups remained within the reported mean range (Table 3).

4 | DISCUSSION

Urolithins, the metabolites produced by colonic microflora during digestion, are known to provide a plenitude of health benefits, as documented in various studies (Liu et al., 2019; Ryu et al., 2016; Vicinanza et al., 2011; Vini et al., 2022; Zhang et al., 2016). The primary metabolites after ingestion of ellagitannin-rich food, found in plasma, tissues, and excreted in urine and feces are UA, UB, and Iso-UA (Giménez-Bastida et al., 2021). In this study, we explored the ability of urolithins, specifically UA and UB, to bind to ER α and counteract the activity of 27-HC. It was found that the antiproliferative activity of UA was greater than that of UB in ER-positive breast cancer cells. UA treatment led to a decrease in cell viability and proliferation when treated alone or in the presence of 27-HC while remaining non-toxic to normal cells such as MCF-10A. Interestingly, our findings revealed that UA reduced the expression of c-Myc, an estrogen-responsive gene that is often overexpressed in various types of cancers. Many anti-estrogenic treatments, including aromatase inhibitors, tamoxifen, and faslodex, have been shown to downregulate MYC mRNA (Green et al., 2016). Notably, PCNA, a vital proliferation biomarker used in the diagnosis and prognosis of breast cancer, was also downregulated upon UA treatment. Furthermore, our molecular docking analysis demonstrated that UA formed hydrogen bonds with HIE 524, similar to E2 as reported earlier (Skledar et al., 2019), and with LEU 387 in the agonist conformation 1GWR. However, there was no noticeable difference in the affinity of UA or UB towards the agonistic and antagonistic conformation of ER α , which cannot predict its agonist or antagonist nature (Puranik et al., 2019).

We further observed that UA induced ERE-luciferase activity, which was in agreement with the findings of Skledar et al. implying that UA may act as an ER α ligand that can bind to classic ERE elements and activate the downstream targets. However, it is important to note that most known estrogen-responsive genes contain permutations of the consensus vitellogenin ERE (vit-ERE; GGTCACagTGACC)

within their regulatory region, and the affinity of ligands would depend on the specific ERE-target sequence. Hence, we used the N-RLUC-hER281–549/G521T-C-RLUC HER sensor to screen SERM activity. UA exhibited partial SERM-like activity, although not as potent as tamoxifen and 27-HC. Meanwhile, UA had an EC50 value of 5.146 μ M, which was close to the value reported by Skelder et al. (5.59 μ M) but higher than the value reported by Larrosa et al.

Additionally, the estrogen-responsive genes TFF1/pS2 were substantially induced by UA treatment. However, no marked changes were observed in PR levels upon UA treatment. This could be ascribed to the fact that pS2 contains palindromic ERE while PR has an ERE half-site upstream of two adjacent Sp1 sites. It is likely that UA binding to ER α might facilitate binding to classical ERE elements but not Sp1 sites, thereby resulting in no meaningful change in PR expression. Nevertheless, further experiments may be required to elucidate the exact mechanism. In addition, the nature of the bound ligand affects ER α stability which probably reflects subtle alterations in receptor conformation. Notably, the degradation of ER α was not observed upon exposure to UA, which was comparable to the action of 4-OHT in stabilizing ER α .

The hollow fiber results were in agreement with the invitro results. The maximum concentration of UA tested in this study was 50 mg/kg bw/d, which is equivalent to 3.8 mg/kg bw/d in humans (Nair & Jacob, 2016). This dosage is much lower than the highest dose of UA tested in humans (Andreux et al., 2019). We found a reduction in cell viability in ER-positive cells placed both subcutaneously and intraperitoneally but with a more pronounced effect in the subcutaneous implants. This could be attributed to the availability of varying metabolites. It is known that drugs administered systemically enter the peritoneal fluid only partially, leading to lower concentrations that may not produce reliable anti-tumor effects in the peritoneal cavity. This is primarily because tumor cell aggregates either remain suspended in the ascites or attach to the peritoneum, and due to the lack of vasculature, drugs carried by the blood cannot reach the tumor cells via the bloodstream (Sugahara et al., 2015). One possible explanation for the observed differences could be investigated by administering UA via direct intraperitoneal injection instead of oral delivery, allowing direct entry into the peritoneal cavity. Surprisingly, despite passing via the gastrointestinal tract, UA retained its antiproliferative effect. The uterine morphometric analysis clearly suggested that UA induced a partial but persistent estrogen-like effect, either alone or in combination with 27-HC.

Furthermore, UA has demonstrated health benefits in cardiovascular, muscular, skeletal, breast, endometrium, and brain tissues, most of which contain ERs playing a vital role. Meanwhile, the exact mechanism underlying the inhibition of breast cancer proliferation by UA needs further investigation. The activity of ERs is complex and dynamic, largely dependent on different conformations influenced by the ligand structure and binding. Herein, we observed that UA exhibited mixed activity in breast cancer cells, establishing ER modulatory properties rather than purely agonistic or antagonistic effects. Given the pleiotropic activity of ERs, it is crucial to thoroughly consider the potential benefits and adverse effects of UA in ER-dependent tissues

TABLE 3 The blood biochemistry parameters of the NOD-SCID mice as evaluated.

Parameters	Reported mean value	Control	OVX control	UA (40 mg/kg/B.W)	UA (50 mg/kg/B.W)	UA (40 mg/kg/B.W + 27-HC)	UA (50 mg/kg/B.W + 27-HC)	27-HC (1 mg/kg/B.W)	E2 (1 mg/kg/B.W)
Total Cholesterol (mg/dL)	63–174	77 ± 8.2	67.6 ± 8.29	67.33 ± 7.64	63.5 ± 3.54	72 ± 9.19	59.5 ± 7.78	63.5 ± 3.54	67 ± 5.66
Triglyceride (mg/dL)	71–164	107 ± 20	110.5 ± 20	86 ± 20.81	70.5 ± 21.92	49 ± 20.42	115 ± 6.6	103 ± 8.49	69.5 ± 10.4
AST/GOT (IU/l)	69–191	84 ± 12	128.8 ± 10	77.33 ± 35.7	187 ± 20	130.5 ± 15.95	90 ± 21.21	102 ± 9.9	155.5 ± 44.55
Alkaline Phosphatase (IU/l)	44–118	36 ± 5.1	35.4 ± 9.56	30.33 ± 4.16	29.5 ± 3.54	28.5 ± 10.97	20 ± 2.83	30 ± 5.14	40.5 ± 2.12
GPT/ALT (IU/l)	26–120	17 ± 6.2	27.2 ± 15.02	18 ± 6.08	21 ± 7	14.5 ± 4.93	24.5 ± 7.68	20 ± 4.24	34 ± 22.63
Total Bilirubin (mg/dL)	0.3–0.8	0.3 ± 0.09	0.42 ± 0.13	0.37 ± 0.06	0.35 ± 0.07	0.5 ± 0.07	0.35 ± 0.07	0.3 ± 0	0.5 ± 0.14
Albumin (g/dL)	2–4.7	2.8 ± 0.12	1.9 ± 0.74	2.33 ± 0.25	2.45 ± 0.07	1.7 ± 0.35	2.2 ± 0	2.3 ± 0.14	2.3 ± 0
Total Protein (g/dL)	4.3–6.5	3.4 ± 0.19	4.58 ± 0.33	3.83 ± 1	4.65 ± 0.21	4.15 ± 0.25	4.35 ± 0.07	4.45 ± 0.35	4.55 ± 0.21
Calcium (mg/dL)	9–12	9 ± 0.16	8.46 ± 0.43	9 ± 0.17	8.5 ± 0.14	8.6 ± 0.12	8.95 ± 1.06	9 ± 0.42	8.65 ± 0.07
BUN (mg/dL)	19–70	40 ± 2.1	45.53 ± 5.17	45.7 ± 1.65	47.2 ± 2.55	44.15 ± 1.1	45.7 ± 0.99	48.75 ± 0.35	35.05 ± 0.92

Note: Blood samples were collected. Sham control and OVX mice implanted with hollow fibers, exposed to 0.1% DMSO, 27-HC (1 mg/kg BW), UA (40 mg/kg BW), UA (40 mg/kg BW + 1 mg/kg BW), UA (50 mg/kg BW + 1 mg/kg BW) for 5 days. Data expressed as mean ± SE. (n = 3). On the day of hollow fiber removal, after sacrificing the animals, various biochemical parameters were analyzed: total cholesterol (mg/dL), triglyceride (mg/dL), AST/SGOT: serum glutamic oxaloacetic transaminase/(AST = aspartate amino transferase); alkaline phosphatase (IU/l) ALT/SGPT: serum glutamic pyruvic transaminase/(ALP = alanine amino transferase); BUN: blood urea nitrogen; CREAT: serum creatinine; LDH: lactate dehydrogenase. The number of animals per group, n = 3.

(Vini et al., 2022). These investigations should be conducted using appropriate *in vivo* models, including long-term treatment studies. Based on the current findings, it appeared that UA has the ability to regulate ER α in breast cancer cells, induce apoptosis, and reduce 27-HC-induced proliferation. Additionally, it exhibited a SERM-like profile. Considering that UA has been extensively studied for its safety and high tolerance (Heilman et al., 2017), this study highlights the potential of UA as an ER modulator and its benefits in estrogen-dependent tissues.

AUTHOR CONTRIBUTIONS

Ravindran Vini: Conceptualization; formal analysis; investigation; writing – original draft. **Vishnu Sunil Jaikumar:** Investigation. **Viji Remadevi:** Investigation. **Juberiya M. Azeez:** Formal analysis. **Anjana Sasikumar:** Investigation. **Swathy Ravindran:** Investigation. **Shankar Sundaram:** Formal analysis. **Sreeharshan Sreeja:** Conceptualization; funding acquisition; supervision; writing – review and editing.

FUNDING INFORMATION

This work was supported by Science and Engineering Research Board (SERB) (EMR/2016/000557) and Department of Biotechnology (DBT) (No. BT/01/CEIB/01/CB/2016). VR and VRD acknowledges the support of ICMR Senior Research Fellowship, Govt of India. We acknowledge Dr. Paul Murugan for donating the pcDNA-N-RLUC-hER281–549-CRLUC plasmid. We also acknowledge the RGCB core facility and the intramural support.

CONFLICT OF INTEREST STATEMENT

The authors declare that they have no conflict of interest with the contents of this article.

DATA AVAILABILITY STATEMENT

All the data generated in this study are included in the manuscript.

ORCID

Ravindran Vini  <https://orcid.org/0000-0002-4756-3674>

Vishnu Sunil Jaikumar  <https://orcid.org/0000-0002-6477-9856>

Sreeharshan Sreeja  <https://orcid.org/0000-0001-7000-6545>

REFERENCES

- Andreux, P. A., Blanco-Bose, W., Ryu, D., Burdet, F., Ibberson, M., Aebischer, P., Auwerx, J., Singh, A., & Rinsch, C. (2019). The mitophagy activator urolithin A is safe and induces a molecular signature of improved mitochondrial and cellular health in humans. *Nature Metabolism*, 1(6), 595–603.
- Asghari, A., & Umetani, M. (2020). Obesity and cancer: 27-hydroxycholesterol, the missing link. *International Journal of Molecular Sciences*, 21(14), 4822.
- Baek, A. E., Krawczynska, N., Das Gupta, A., Dvoretzkiy, S. V., You, S., Park, J., Deng, Y. H., Sorrells, J. E., Smith, B. P., Ma, L., & Nelson, E. R. (2021). The cholesterol metabolite 27-HC increases secretion of extracellular vesicles promote breast cancer progression. *Endocrinology*, 162(7), bqab095.
- Baek, A. E., Yu, Y. R. A., He, S., Wardell, S. E., Chang, C. Y., Kwon, S., Pillai, R. V., McDowell, H. B., Thompson, J. W., Dubois, L. G., &

- Nelson, E. R. (2017). The cholesterol metabolite 27-hydroxycholesterol facilitates breast cancer metastasis through its actions on immune cells. *Nature Communications*, 8(1), 1–11.
- Chen, R., Guo, S., Yang, C., Sun, L., Zong, B., Li, K., Liu, L., Tu, G., Liu, M., & Liu, S. (2020). Although c-MYC contributes to tamoxifen resistance, it improves cisplatin sensitivity in ER-positive breast cancer. *International Journal of Oncology*, 56(4), 932–944.
- Dias, I. H. K., Brown, C. L., Kiran Shabir, M., Polidori, C., & Griffiths, H. R. (2018). miRNA 933 expression by endothelial cells is increased by 27-hydroxycholesterol and is more prevalent in plasma from dementia patients. *Journal of Alzheimer's Disease*, 64(3), 1009–1017.
- DuSelle, C. D., Umetani, M., Shaul, P. W., Mangelsdorf, D. J., & McDonnell, D. P. (2008). 27-hydroxycholesterol is an endogenous selective estrogen receptor modulator. *Molecular Endocrinology*, 22(1), 65–77.
- Frasor, J., Stossi, F., Danes, J. M., Barry Komm, C., Lyttle, R., & Katzenellenbogen, B. S. (2004). Selective estrogen receptor modulators: Discrimination of agonistic versus antagonistic activities by gene expression profiling in breast cancer cells. *Cancer Research*, 64(4), 1522–1533.
- Gao, F. Y., Li, X. T., Xu, K., Wang, R. T., & Guan, X. X. (2023). c-MYC mediates the crosstalk between breast cancer cells and tumor microenvironment. *Cell Communication and Signaling*, 21(1), 28.
- García-Villalba, R., Selma, M. V., Espín, J. C., & Tomás-Barberán, F. A. (2019). Identification of novel urolithin metabolites in human feces and urine after the intake of a pomegranate extract. *Journal of Agricultural and Food Chemistry*, 67(40), 11099–11107.
- Gibson, D. A., Collins, F., Cousins, F. L., Zufiaurre, A. E., & Saunders, P. T. K. (2018). The impact of 27-hydroxycholesterol on endometrial cancer proliferation. *Endocrine-Related Cancer*, 25(4), 381–391.
- Giménez-Bastida, J. A., Ávila-Gálvez, M. Á., Espín, J. C., & González-Sarrías, A. (2021). Evidence for health properties of pomegranate juices and extracts beyond nutrition: A critical systematic review of human studies. *Trends in Food Science & Technology*, 114, 410–423.
- Green, A., Aleskandarany, M., Agarwal, D., Elsheikh, S., Nolan, C. C., Díez-Rodríguez, M., Macmillan, R. D., Ball, G. R., Caldas, C., Madhusudan, S., & Ellis, I. O. (2016). MYC functions are specific in biological subtypes of breast cancer and confers resistance to endocrine therapy in luminal tumours. *British Journal of Cancer*, 114, 917–928. <https://doi.org/10.1038/bjc.2016.46>
- Guan, J., Zhou, W., Hafner, M., Blake, R. A., Chalouni, C., Chen, I. P., De Bruyn, T., Giltneane, J. M., Hartman, S. J., Heidersbach, A., & Metcalfe, C. (2019). Therapeutic ligands antagonize estrogen receptor function by impairing its mobility. *Cell*, 178(4), 949–963.
- Heilman, J., Andreux, P., Tran, N., Rinsch, C., & Blanco-Bose, W. (2017). Safety assessment of Urolithin A, a metabolite produced by the human gut microbiota upon dietary intake of plant derived ellagitannins and ellagic acid. *Food and Chemical Toxicology*, 108, 289–297.
- Hollingshead, M. G., Alley, M. C., Camalier, R. F., Abbott, B. J., Mayo, J. G., Malspeis, L., & Grever, M. R. (1995). In vivo cultivation of tumor cells in hollow fibers. *Life Sciences*, 57(2), 131–141.
- Ismail, M.-A.-M., Mateos, L., Maioli, S., Merino-Serra, P., Ali, Z., Lodeiro, M., Westman, E., Leitersdorf, E., Gulyás, B., Olof-Wahlund, L., & Winblad, B. (2017). 27-hydroxycholesterol impairs neuronal glucose uptake through an IRAP/GLUT4 system dysregulation. *Journal of Experimental Medicine*, 214(3), 699–717.
- Jurikova, M., Danihel, Ľ., Polák, Š., & Varga, I. (2016). Ki67, PCNA, and MCM proteins: Markers of proliferation in the diagnosis of breast cancer. *Acta Histochemica*, 118(5), 544–552.
- Kim, D., Lee, K. M., Lee, C., Jo, Y. S., Muradillaevna, M. S., Kim, J. H., Yoon, J. H., & Song, P. (2021). Pathophysiological role of 27-hydroxycholesterol in human diseases. *Advances in Biological Regulation*, c83, 100837.
- Kocanova, S., Mazaheri, M., Caze-Subra, S., & Bystricky, K. (2010). Ligands specify estrogen receptor alpha nuclear localization and degradation. *BMC Cell Biology*, 11(1), 1–13.
- Larrosa, M., González-Sarrías, A., García-Conesa, M. T., Tomás-Barberán, F. A., & Espín, J. C. (2006). Urolithins, ellagic acid-derived metabolites produced by human colonic microflora, exhibit estrogenic and antiestrogenic activities. *Journal of Agricultural and Food Chemistry*, 54(5), 1611–1620.
- Larrosa, M., Tomás-Barberán, F. A., & Espin, J. C. (2006). The dietary hydrolysable tannin punicalagin releases ellagic acid that induces apoptosis in human colon adenocarcinoma Caco-2 cells by using the mitochondrial pathways. *Journal of Nutritional Biochemistry*, 17, 611–625.
- Lee, H. Y., Cha, J., Kim, S. K., Park, J. H., Song, K. H., Kim, P., & Kim, M.-Y. (2019). c-MYC drives breast cancer metastasis to the brain, but promotes synthetic lethality with TRAIL. *Molecular Cancer Research*, 17(2), 544–554.
- Lee, S., & Barron, M. G. (2017). Structure-based understanding of binding affinity and mode of estrogen receptor α agonists and antagonists. *PLoS One*, 12(1), e0169607.
- Lee, W.-R., Ishikawa, T., & Umetani, M. (2014). The interaction between metabolism, cancer and cardiovascular disease, connected by 27-hydroxycholesterol. *Clinical Lipidology*, 9(6), 617–624.
- Liu, L., Li, M. Y., Xing, Y., Wang, X. Y., & Wang, Y. (2019). The oncogenic roles of 27-hydroxycholesterol in glioblastoma. *Oncology Letters*, 18(4), 3623–3629.
- Ma, L., Wang, L., Nelson, A. T., Han, C., He, S., Henn, M. A., Menon, K., Chen, J. J., Baek, A. E., Vardanyan, A., & Nelson, E. R. (2020). 27-hydroxycholesterol acts on myeloid immune cells to induce T cell dysfunction, promoting breast cancer progression. *Cancer Letters*, 493, 266–283.
- Ma, R., Zhu, K., Yuan, D., Gong, M., Li, Y., Li, K., & Meng, L. (2021). Down-regulation of the FBXO43 gene inhibits tumor growth in human breast cancer by limiting its interaction with PCNA. *Journal of Translational Medicine*, 19(1), 1–12.
- Mbaveng, A. T., Bitchagno, G. T., Kuete, V., Tane, P., & Efferth, T. (2019). Cytotoxicity of ungeremine towards multi-factorial drug resistant cancer cells and induction of apoptosis, ferroptosis, necroptosis and autophagy. *Phytomedicine*, 60, 152832.
- Mottamal, M., Kang, B., Peng, X., & Wang, G. (2021). From pure antagonists to pure degraders of the estrogen receptor: Evolving strategies for the same target. *ACS Omega*, 6(14), 9334–9343.
- Nair, A. B., & Jacob, S. (2016). A simple practice guide for dose conversion between animals and humans. *J Basic Clin Pharm.*, 7(2), 27–31.
- Nelson, E. R. (2018). The significance of cholesterol and its metabolite, 27-hydroxycholesterol, in breast cancer. *Molecular and Cellular Endocrinology*, 466, 73–80.
- Nelson, E. R., DuSelle, C. D., Wang, X., Howe, M. K., Evans, G., Michalek, R. D., Umetani, M., Rathmell, J. C., Khosla, S., Gesty-Palmer, D., & McDonnell, D. P. (2011). The oxysterol, 27-hydroxycholesterol, links cholesterol metabolism to bone homeostasis through its actions on the estrogen and liver X receptors. *Endocrinology*, 152(12), 4691–4705.
- Paulmurugan, R., & Gambhir, S. S. (2006). An intramolecular folding sensor for imaging estrogen receptor–ligand interactions. *Proceedings of the National Academy of Sciences of the United States of America*, 103(43), 15883–15888.
- Petz, L. N., Ziegler, Y. S., Schultz, J. R., Hwajin Kim, J., Kemper, K., & Nardulli, A. M. (2004). Differential regulation of the human progesterone receptor gene through an estrogen response element half-site and Sp1 sites. *The Journal of Steroid Biochemistry and Molecular Biology*, 88(2), 113–122.
- Puranik, N. V., Srivastava, P., Bhatt, G., John Mary, D. J. S., Limaye, A. M., & Sivaraman, J. (2019). Determination and analysis of agonist and antagonist potential of naturally occurring flavonoids for

- estrogen receptor (ER α) by various parameters and molecular modeling approach. *Scientific Reports*, 9(1), 1–11.
- Revilla, G., de Pablo, M., Pons, L. B.-R., García-León, A., Santos, D., Cenarro, A., Magalhaes, M., et al. (2019). Cholesterol and 27-hydroxycholesterol promote thyroid carcinoma aggressiveness. *Scientific Reports*, 9(1), 1–13.
- Ryu, D., Mouchiroud, L., Andreux, P. A., Katsyuba, E., Moullan, N., Nicolet-dit-Félix, A. A., Williams, E. G., Jha, P., Lo Sasso, G., Huzard, D., & Auwerx, J. (2016). Urolithin A induces mitophagy and prolongs lifespan in *C. elegans* and increases muscle function in rodents. *Nature Medicine*, 22(8), 879–888. <https://doi.org/10.1038/nm.4132> Epub 2016 Jul 11. PMID: 27400265.
- Singh, A., D'Amico, D., Andreux, P. A., Fouassier, A. M., Blanco-Bose, W., Evans, M., Aebischer, P., Auwerx, J., & Rinsch, C. (2022). Urolithin A improves muscle strength, exercise performance, and biomarkers of mitochondrial health in a randomized trial in middle-aged adults. *Cell Reports Medicine*, 3(5), 100633. <https://doi.org/10.1016/j.xcrm.2022.100633> PMID: 35584623; PMCID: PMC9133463.
- Skledar, D. G., Tomašič, T., Dolenc, M. S., Mašič, L. P., & Zega, A. (2019). Evaluation of endocrine activities of ellagic acid and urolithins using reporter gene assays. *Chemosphere*, 220, 706–713.
- Sreeja, S., Kumar, T. R. S., Lakshmi, B. S., & Sreeja, S. (2012). Pomegranate extract demonstrates a selective estrogen receptor modulator profile in human tumor cell lines and in vivo models of estrogen deprivation. *The Journal of Nutritional Biochemistry*, 23(7), 725–732.
- Sreekumar, S., Sithul, H., Muraleedharan, P., Azeez, J. M., & Sreeharshan, S. (2014). Pomegranate fruit is a rich source of biologically active compounds. *BioMed Research International*, 2014, 686921.
- Sugahara, K. N., Scodeller, P., Braun, G. B., De Mendoza, T. H., Yamazaki, C. M., Kluger, M. D., ... Lowy, A. M. (2015). A tumor-penetrating peptide enhances circulation-independent targeting of peritoneal carcinomatosis. *Journal of Controlled Release*, 212, 59–69.
- Umetani, M., Domoto, H., Gormley, A. K., Yuhanna, I. S., Cummins, C. L., Javitt, N. B., Korach, K. S., Shaul, P. W., & Mangelsdorf, D. J. (2007). 27-hydroxycholesterol is an endogenous SERM that inhibits the cardiovascular effects of estrogen. *Nature Medicine*, 13(10), 1185–1192.
- Vicinanza, R., Zhang, Y., Henning, S. M., Li, Z., & Heber, D. (2011). Urolithin A and ellagic acid inhibit prostate cancer through different molecular mechanisms: Implications of gut microbiome metabolism for cancer prevention.
- Vini, R., Juberiya, A. M., & Sreeja, S. (2016). Evidence of pomegranate methanolic extract in antagonizing the endogenous SERM, 27-hydroxycholesterol. *IUBMB Life*, 68(2), 116–121.
- Vini, R., Rajavelu, A., & Sreeharshan, S. (2022). 27-hydroxycholesterol, the estrogen receptor modulator, alters DNA methylation in breast cancer. *Frontiers in Endocrinology*, 13, 783823.
- Wu, Q., Ishikawa, T., Sirianni, R., Tang, H., McDonald, J. G., Yuhanna, I. S., Thompson, B., Girard, L., Mineo, C., Brekken, R. A., & Umetani, M. (2013). 27-hydroxycholesterol promotes cell-autonomous, ER-positive breast cancer growth. *Cell Reports*, 5(3), 637–645.
- Zhang, W., Chen, J. H., Aguilera-Barrantes, I., Shiau, C. W., Sheng, X., Wang, L. S., ... Huang, Y. W. (2016). Urolithin A suppresses the proliferation of endometrial cancer cells by mediating estrogen receptor- α -dependent gene expression. *Molecular Nutrition & Food Research*, 60(11), 2387–2395.

How to cite this article: Vini, R., Jaikumar, V. S., Remadevi, V., Ravindran, S., Azeez, J. M., Sasikumar, A., Sundaram, S., & Sreeja, S. (2023). Urolithin A: A promising selective estrogen receptor modulator and 27-hydroxycholesterol attenuator in breast cancer. *Phytotherapy Research*, 1–18. <https://doi.org/10.1002/ptr.7919>